An efficient ice-sheet/Earth system model spin-up procedure for CESM2.1 and CISM2.1: description, evaluation, and broader applicability

Marcus Lofverstrom[1,2], Jeremy Fyke[3,4], Katherine Thayer-Calder[2], Laura Muntjewerf[5], Miren Vizcaino[5], William J. Sacks[2], William H. Lipscomb[2], Bette Otto-Bliesner[2], Sarah L. Bradley[5,6]

[1]University of Arizona
[2]Climate and Global Dynamics Laboratory, National Center for Atmospheric Research
[3]Associated Engineering Group, Ltd.
[4]University of Colorado
[5]Delft University of Technology
[6]The University of Sheffield

Key Points:

- Computationally tractable method for spinning up a coupled ice sheet/Earth system model
- Model equilibrium climate is similar to traditional spinup simulation with prescribed ice sheets
- A novel iterative spinup procedure of fully coupled Earth system models

Corresponding author: Marcus Lofverstrom, `lofverstrom@arizona.edu`

Abstract

Spinning up a fully coupled Earth system model is a time consuming and computationally demanding exercise. For models with interactive ice-sheet components, this becomes a major challenge, as ice sheets are sensitive to bi-directional feedback processes and equilibrate over glacial timescales of up to many millennia. This work describes and demonstrates a computationally tractable, iterative procedure for spinning up a comprehensive Earth system model that includes an ice sheet component. The procedure alternates between a computationally expensive fully coupled configuration and a computationally cheaper configuration where the atmospheric component is replaced by a data model. By periodically regenerating atmospheric forcing consistent with the coupled system, the data atmosphere remains adequately constrained to ensure that the broader model state evolves realistically. The applicability of the method is demonstrated by spinning up the pre-industrial climate in the Community Earth System Model version 2 (CESM2), coupled to the Community Ice Sheet Model version 2 (CISM2) over Greenland. The equilibrium climate is similar to the control climate from a fully coupled simulation with a prescribed Greenland ice sheet, indicating that the iterative procedure is consistent with a traditional spinup approach without interactive ice sheets. These results suggest that the iterative method can provide a faster and cheaper method for spinning up fully coupled Earth system model, with or without interactive ice-sheet components. The equilibrium climate/ice-sheet state will serve as initial conditions for transient fully-coupled historical and future simulations with CESM2-CISM2 in the Coupled Model Intercomparison Project phase 6 (CMIP6).

Plain Language Summary

Experiments with Earth system models often use the pre-industrial (1850 CE) climate as reference point when examining the climate response to a given experiment scenario. The pre-industrial climate is therefore important to represent consistently, which often requires long simulations to ensure that the model climate is in balance. The latest generation Earth system models include time-evolving ice sheet components, which add substantial complexity to the task of generating a simulated pre-industrial climate in approximate balance. This is because ice sheets interact with the rest of the climate system through a range of complex processes, and also because they respond slowly to climate change and at the whole ice sheet scale equilibrate over multi-millennial timescales. Here we present a novel method for generating an internally consistent climate state that is particularly suitable for models with interactive ice sheet components. The method described yields substantial resource savings compared to more traditional simulations methods, while simultaneously generating a climate that is consistent with more computationally expensive methods. The viability of the method is demonstrated by generating the pre-industrial control climate in the Community Earth System Model version 2 (CESM2), which includes a fully interactive representation of the Greenland ice sheet.

Keywords: Community Earth System Model version 2 (CESM2); Coupled ice-sheet/Earth system modeling; Interactive ice sheets; Spinup simulation

1 Introduction

Continental-scale ice sheets are integral parts of the Earth system, which directly and indirectly interact with other components of the Earth system over a range of different time scales; see the recent review by Fyke et al. (2018). At present there are two ice sheets on the planet: the Antarctic Ice Sheet (AIS; ice volume around 58 m global-mean sea-level equivalent; Fretwell et al., 2013) in the Southern Hemisphere, and the Greenland Ice Sheet (GrIS; ice volume around 7 m global-mean sea-level equivalent; Morlighem et al., 2017) in the Northern Hemisphere. These ice sheets are potentially highly suscep-

tible to anthropogenic climate change, which is enhanced at high latitudes (so-called *polar amplification*) by internal feedback processes in the climate system (e.g. Serreze & Francis, 2006; Graversen et al., 2008; D. M. Smith et al., 2019). Satellite-based monitoring programs indicate that both the GrIS and AIS have been losing mass at an accelerated rate in the last few decades, and they are currently contributing about 1 mm to global sea-level rise each year (Rignot & Kanagaratnam, 2006; Van den Broeke et al., 2016; Rignot et al., 2019). Understanding the bi-directional climate–ice-sheet coupling and sensitivity is thus a high priority for ongoing and future research that aims to improve sea level rise projections, impact assessments, and adaptation planning (Fyke et al., 2018).

Historically, Earth system models (ESMs) have largely represented ice sheets as prescribed (or passive) "white mountains", which interact with the circulation through topography, albedo, and surface snow effects, but do not themselves respond to the simulated climate. However, several major modeling centers have started incorporating fully interactive thermo-mechanical ice-sheet components into their ESMs — notably, models participating in the Ice Sheet Model Intercomparison Project (ISMIP6) (Nowicki et al., 2016) under the auspice of the Coupled Model Intercomparison Project (CMIP6) (Eyring et al., 2016). The newly released Community Earth System Model, version 2 (CESM2) (Danabasoglu et al., in review), from the National Center for Atmospheric Research (NCAR), is one of the first comprehensive ESMs to include fully interactive (or two-way) coupling between a dynamic ice sheet model of the GrIS (Lipscomb et al., 2019) and the broader Earth system model (Muntjewerf, in preparation).

The realism of the equilibrated pre-industrial climate (typically year 1850 CE), as well as historical transient simulations over the instrument era (commonly from 1850 CE to modern), have long been important benchmarks for assessing the overall quality of coupled climate models. The pre-industrial climate also often serves as initial condition for experiments with perturbed forcing protocols (e.g., Eyring et al., 2016), as it is desirable to start from an internally consistent model state that is free from residual unrealistic drift. Including a fully interactive ice-sheet component adds considerable complexity to the spinup procedure.

First of all, ice sheets have large thermal and dynamic inertia and thus respond slowly to imposed climate forcing. Standalone ice-sheet model simulations of the GrIS typically reach steady state in around 10,000 years (a similar timescale as the average residence time in ice sheets; see Section 4) when run under a constant forcing protocol (e.g. Stone et al., 2010; Koenig et al., 2015). This is even longer than the equilibrium timescales of deep ocean biogeochemical tracers and the soil carbon and nitrogen pools (Thornton & Rosenbloom, 2005; Ilyina et al., 2013), which traditionally have been the major bottlenecks when spinning up ESMs.

Ice sheets are also sensitive to both direct and indirect bi-directional ice-sheet/Earth system feedback processes (Fyke et al., 2018) that can strongly influence their growth trajectories, height, extent, and morphology (e.g. Ridley et al., 2005; DeConto et al., 2007). Feedbacks can generate complex and counter-intuitive behavior; for example, ice growth in one region can result in stagnation, or even retreat in other areas from feedback-induced changes to local climate conditions (see paleo-climate examples in Lofverstrom et al., 2015; Lofverstrom & Liakka, 2016).

A consequence of complicated ice-sheet/Earth system coupling is that purely uncoupled methods (i.e., standalone ice-sheet model simulations) tend to struggle when applied to the generation of self-consistent coupled ice-sheet/Earth system conditions. This is because spurious transients — both in the ice sheet and in the other model components — emerge when a standalone ice sheet instance is reintroduced into a coupled model setting. Moreover, ice-sheet dynamics are influenced by the internal ice temperature structure, as cold ice is more viscous than warmer ice and is thus more resistant to gravita-

tional deformation — sliding properties are in turn regulated by basal temperatures. When the bottom of the firn layer is compressed into ice, the in-situ temperature is "archived" in the ice sheet. As new annual layers form, the thermal memory of past climates is recorded vertically through the ice column. In other words, the ice dynamics today is (at least to some degree) influenced by the evolution of the Greenland climate as far back as the last glacial period. This information should ideally be accounted for to obtain realistic rheology and flow dynamics.

Given these physical restrictions, an ideal coupled climate–ice-sheet model spin-up would entail a transient simulation over the entire Last Glacial Cycle. Although this would be ideal for capturing ice-sheet/climate feedback processes and long whole-ice sheet response times, it is computationally infeasible to run an ESM for more than a few centuries (see Tables 1 and 2). One method to reduce the computational cost is to accelerate the ice sheet (i.e., asynchronous coupling) with respect to the other model components (e.g. Ridley et al., 2005; Ziemen et al., 2019). This approach leverages the fact that year-to-year changes in ice-sheet area and topography are typically small, even at the edges where the ice sheet is highly dynamic with fast outlet glaciers and pronounced summer ablation. Accelerating the ice-sheet component is thus an attractive solution to reduce the overall integration length of coupled models. However, even with reasonable acceleration factors (Ganopolski et al., 2010), simple asynchronous acceleration can still be computationally infeasible for comprehensive coupled models (Table 2), especially for repeated simulations (e.g., sensitivity or perturbed initial condition ensembles).

Building on the concept of asynchronous acceleration, here we present a novel iterative procedure for spinning up a coupled climate model state, targeted at computational requirements, configurations, and designs of the Community Earth System Model (CESM2). This method is particularly suited for computationally expensive models with an interactive ice-sheet component. The method is designed to satisfy the following goals and requirements as well as possible:

(i) All model components are allowed to evolve and equilibrate in a coupled fashion to account for bi-directional feedback processes, including bi-directional ice-sheet/climate feedback processes that regulate ice sheet evolution.
(ii) The final result is an internally consistent climate state where all model components are in statistical equilibrium (or in a non-equilibrium state that is consistent with prior climate history; e.g. the Last Glacial Cycle, in the case of ice sheets).
(iii) The equilibrium climate is similar to that obtained using a standard spin-up technique of a fully coupled ESM with a prescribed ice sheet geometry.
(iv) The technique is feasible for model equilibration, given available computing resources.

We have developed and applied a method that satisfies these goals in the course of developing a feasible ice-sheet/Earth system modeling and analysis workflow within CESM2. Given commonalities between CESM2 and other ESMs (Alexander & Easterbrook, 2015), the technique may prove useful in reducing the computational cost of spinning other coupled model frameworks, even in lieu of interactive ice sheet model additions.

The paper is organized as follows: The model and experiment design are presented in sections 2, 3, and 4. The iterative method is demonstrated in section 5, followed by a general discussion and conclusions in sections 6 and 7.

2 Model Description

The Community Earth System Model (CESM) is a state-of-the-art, fully-coupled global Earth system model, primarily developed and administered at the National Cen-

ter of Atmospheric Research (NCAR). CESM2 (Danabasoglu et al., in review) is the newest member of the CESM model family, and will contribute simulations of past, present, and future climates to the Coupled Model Intercomparison project (CMIP6) (Eyring et al., 2016), which is one of the central modeling initiatives of modern climate science (e.g., it plays and important role for the upcoming sixth assessment report from the IPCC; https://www.ipcc.ch/assessment-report/ar6/).

CESM2 consists of prognostic components of atmosphere, land, river, ocean, ocean surface waves, sea ice, and land ice; see Danabasoglu et al. (in review) and http://www.cesm.ucar.edu/models/ces for an exhaustive description of the model and its performance. Recent model improvements with significance for the present study are described in the following.

The Community Atmosphere Model (CAM6; Neale et al., personal communication) has adopted the Beljaars et al. (2004) form drag parameterization and a new anisotropic orographic gravity wave scheme that accounts for the orientation of sub-grid-scale ridges and low-level blocking. This has substantially improved precipitation on the ice sheet edges, and also improved turbulent energy fluxes in the boundary layer, which are important components of the surface mass balance.

The Community Land Model (CLM5) (Lawrence et al., 2019) contains substantially improved snow physics to account for temperature and wind-driven compaction, and the inclusion of a firn model (van Kampenhout et al., 2017) that allows for a more realistic meltwater infiltration and refreezing (the snow pack has been increased to 12 levels with a maximum depth of 10 m liquid water equivalent).

The Community Ice Sheet Model (CISM2.1; Lipscomb et al., 2019), has a parallel, higher-order velocity solver (Goldberg, 2011) that realistically simulates slow interior flow as well as fast flow in ice streams and outlet glaciers. Parameterizations of basal sliding (Aschwanden et al., 2016), iceberg calving, and other physical processes have been improved from earlier versions of the model. Surface temperature and surface mass balance (SMB) are computed in the land model (CLM5) in multiple elevation classes for each glaciated grid cell (Lipscomb et al., 2013; Sellevold et al., 2019). Over the GrIS, these fields are downscaled to the higher resolution (4-km) CISM2 grid. The initial interpolation is bilinear in the horizontal and linear (between adjacent elevation classes) in the vertical. A global correction factor is then applied so that the total accumulation and ablation computed in CLM5 are equal to the accumulation and ablation applied in CISM2. No downscaling is currently applied for Antarctica and smaller mountain glaciers since their geometries remain prescribed. CISM2 also includes an active isostasy model, with an elastic lithosphere and relaxing asthenosphere (with a relaxation timescale of 3000 years) as described in Rutt et al. (2009). Floating ice shelves are not modeled explicitly; instead, ice calves as soon as it becomes afloat. We consider this a reasonable simplification for the GrIS, but it would not be appropriate for the AIS.

CESM2 has bi-directionally active ice-sheet–land–atmosphere–ocean coupling (Muntjewerf, in preparation) (the ice-sheet model is currently one-way coupled to the ocean component), including an energy-based mass-balance scheme to represent realistic variations in accumulation and ablation, and interactive land-surface types (vegetated and glaciated landunits — bare ground is prescribed under the modern observed GrIS extent, while tundra is prescribed around the periphery) as the GrIS advances and retreats. When CLM5 is run interactively with CISM2, snow accumulation that exceeds the 10 m maximum allowed snow depth in the ice-sheet domain (i.e., Greenland) is added to the top of CLM5's snow pack, and an equivalent amount at the bottom of the snow pack is converted to ice and passed as a positive SMB to the ice sheet. Melting of the CLM5 ice column in the ice-sheet domain is communicated to CISM2 as a negative SMB, with meltwater runoff routed from CLM5 to the ocean (Parallel Ocean Model; POP2) (Smith et al., 2010) by the river model (Model for Scale Adaptive River Transport; MOSART) (Tesfa et al., 2014). Outside the ice-sheet domain, solid runoff from excess snow in CLM5 is routed to the

POP2 by MOSART, where it is melted (by the ocean) and spread diffusively. This treatment of solid runoff also applies to the default setup without interactive ice sheets.

Further, the ice sheet model sends calving fluxes to the ocean as solid ice runoff, and sends basal melting fluxes from grounded ice (usually small in comparison to surface melting and calving fluxes) as liquid runoff. In the current model, basal melting of floating ice shelves is not included. Freshwater and salinity are conserved in the model, but eustatic sea-level change is not explicitly simulated by changes in the land-ocean distribution. More details on CLM5-CISM2 coupling can be found in Muntjewerf (in preparation) and Leguy et al. (2019).

All model components are dynamically coupled and exchange state information via a coupler that conservatively interpolates fields between the different model domains. The atmosphere (CAM6) and land (CLM5) models run on a $0.9° \times 1.25°$ finite volume grid, the ocean (POP2) model and Community Sea ice Model (CICE5) use a nominal $1°$ resolution rotated pole grid, and the ice-sheet component (CISM2) runs on a limited-area 4×4 km grid centred over Greenland.

2.1 Component sets

The CESM2 infrastructure supports a large variety of model configurations and forcing protocols, ranging from standalone experiments with individual modelled Earth system components (generally forced by observational or reanalysis datasets), to fully coupled simulations that include all Earth system components, where the model climate is determined internally under imposed planetary boundary conditions. These model configurations, commonly referred to as component sets or *compsets*, are configured by a combined user interface/control system called the Common Infrastructure for Modeling the Earth (CIME; http://esmci.github.io/cime/). The method described here relies importantly on the use of multiple compsets, each of which is described below.

2.1.1 BG component set

The BG compset consists of the fully coupled model with a two-way interactive ice sheet. Here, *B* denotes fully coupled CESM2, and *G* denotes an interactive ice sheet. This is the most comprehensive way of running CESM2, where all components are interactive and coupled. This is also the most computationally expensive type of simulation (Table 1), though including the interactive ice-sheet model only adds about 1% to the total integration cost of the fully-coupled model (i.e., relative to the B compset).

2.1.2 JG component set

As part of this methodology, a new component set (*JG compset*) was introduced. The JG compset is similar to the fully coupled BG compset, but with CAM6 replaced by a computationally inexpensive data atmosphere. With an optimized processor layout, throughput (i.e., simulated model years per day) for the JG compset is more than four times greater than for the BG compset, and the computational cost is reduced by a factor of three (Table 1).

The JG compset allows for two-way coupling between CISM2 and all other model components except for the prescribed data atmosphere. Most importantly, this allows ice sheet meltwater runoff and calving to interact with the ocean during convergence to steady state. However, similar to standalone ocean model simulations, we apply a weak (timescale of 1 year) restoring of the sea-surface salinity field to suppress spurious drift in the overturning circulation from runaway feedbacks with a prescribed atmospheric state (e.g., Griffies et al., 2009, 2016).

2.1.3 T component set

The ice-sheet component (CISM2.1) can be run as a free-standing (i.e., *ice-sheet-only*) model within the CIME infrastructure using the *T compset*. In this configuration, SMB and surface temperature on multiple elevation classes are downscaled to CISM2 to account for elevation feedbacks when the ice sheet evolves. Typically, the surface forcing is provided by a previous run with an active land model. The computational cost of the T compset is low compared to the BG and JG compsets, allowing for multi-millennial simulations within a wall-clock day. The T compset simulations described here were driven with prescribed boundary conditions from BG segments of the procedure.

2.2 Dynamic topography updating

In the standard implementation of CESM2, a time-invariant topography used by the atmosphere model (CAM6) is prescribed and read from an external file when the model simulation is initialized. In standard configuations without interactive ice sheets, this is acceptable. However, it introduces an inconsistency when running with interactive CISM2 as the ice-sheet topography changes over time. Updating the CAM6 topography continually at run time is not computationally feasible, as information about sub-gridscale topography variance and ridge orientation (used in orographic drag and gravity wave parameterizations in the planetary boundary layer) is derived from a high-resolution global dataset using algorithms that are not included in run-time CAM6 operation.

Thus, as part of the experiments presented here, an offline tool was developed that periodically updates the topography boundary condition in CAM6, to include changes in the ice-sheet topography. The workflow is as follows:

(i) At the completion of each run segment, atmosphere and (GrIS) ice sheet states are written to standard restart files.
(ii) The ice-sheet topography is extracted from the CISM2 restart file, regridded to a 30-second grid (approximately 1 km resolution) and overlaid onto the GMTED2010 dataset (Global Multi-resolution Terrain Elevation Data 2010; Danielson & Gesch, 2011), which forms the basis for the CAM6 topography.
(iii) The CAM6 topography generation routine (Lauritzen et al., 2015) is then run in its entirety. This includes remapping of the modified GMTED2010 topography to a 3-km cubed sphere grid, from which the sub-gridscale topography variance and ridge orientation is derived. The topography is then smoothed and interpolated back to the CAM6 model resolution.
(iv) The new global, smoothed CAM6 topography and subgrid roughness fields, which incorporate the altered CISM2 topography, are re-inserted into the CAM6 restart and topography files. (The topography updating routine is not officially supported in the CESM2 model distribution. Consequently, topography fields that were used in previous model versions (PHIS, SGH, and SGH30) are read from the restart file, while information about ridge orientation and the sub-gridscale variance fields used in the new surface drag parameterisations are read from the topography dataset).
(v) CESM2 is then automatically re-submitted.

3 Model spin-up procedure

The primary objective of spinning up (or equilibrating) an ESM is to generate an internally consistent coupled Earth system state, where all model components are in a statistical equilibrium — a state which reflects balance between all inter-component interactions and feedbacks. The length of a model spin-up is determined by the effective equilibration time of included Earth system components. In the absence of ice sheets, equilibration times are typically set by abyssal ocean and soil conditions, which can carry

traces of past climate conditions for several millennia. Inclusion of a fully interactive ice sheet component complicates the exercise further, since ice sheets can carry a dynamic and thermodynamic memory spanning well over 10 kyr. This makes ice sheets the Earth system component with the longest equilibration time, by a notable margin.

In contrast, the atmosphere has almost no memory and adjusts quickly to altered conditions. This means that atmospheric model components of coupled ESMs are essentially "carried along for the ride", as slower-responding components equilibrate. In the case of CESM2, the atmosphere component (CAM6) accounts for about 70% of the total model cost at the standard 1-degree resolution, and is thus by far the most computationally expensive component of the coupled model (the exact percentage being dependent on external factors such as computer architecture, total CPU count, and load balancing). Substantial computational savings can therefore potentially be made by minimizing atmosphere model cycles, while still allowing all model components to evolve in a coupled fashion. In particular, we assume that if the model climate is in quasi-equilibrium (i.e., "small" drift, for example defined by a small ratio of drift signal to forced signal), the atmospheric component can theoretically be prescribed for extended periods of time without significantly impacting the spin-up trajectory of components with a higher inertia or equilibration timescales. However, to regain consistency with a fully coupled simulation, the atmospheric state — which is effectively a boundary condition in the other model components in the JG compset — has to be updated periodically via fully coupled simulations, to allow atmospherically-regulated changes in the overall coupled model state to evolve realistically.

Leveraging this set of assumptions, the spin-up procedure iterates between two simulation types: the fully coupled BG compset (section 2.1.1), where all model components are active and dynamically interacting; and the JG compset (section 2.1.2), where the atmosphere model is replaced by a prescribed data model. The estimated running costs of these model configurations (at the nominal 1-degree horizontal resolution) are presented in Table 1.

The workflow of the spin-up procedure is as follows (see also schematic illustration in Fig. 1):

(i) A fully coupled (BG) simulation is run for 35 model years, using full synchronous climate–ice-sheet coupling. The first 5 years of the data is discarded for the first and all subsequent BG simulation iterations (i.e, we only consider data from the last 30 model years), to remove any initial spurious transient behavior in the atmospheric state resulting from the iterative procedure. During this stage, instantaneous high frequency atmospheric data is extracted from the coupler and written to external files. (30 years was chosen as a compromise between simulation cost and accuracy, and to ensure that several cycles of naturally occurring modes of variability are represented in the data archive). Data consists of hourly frequency longwave & shortwave surface radiation, and near-surface horizontal (u & v) wind, as well as 3-hourly frequency surface temperature, pressure, precipitation, and near surface (evaluated at lowest model level) potential temperature, specific humidity, density, elevation, and pressure.

(ii) Next, a JG compset simulation is run, where the atmosphere model is replaced by the high-frequency data archive generated from the preceding fully coupled simulation. The 30 years of atmosphere data is cycled 5 times, for a total integration length of 150 model years for the ocean, land, and sea-ice components. Concurrently, the ice-sheet component is accelerated by a factor of 10, for a total of 1500 simulated ice-sheet years. The ocean surface salinity relaxation (described in section 2.1.2) uses climatological data from the preceding fully-coupled simulation. At the end of the JG simulation, the topography dataset used by the atmospheric

model in the BG simulation is updated (see section 2.2) to incorporate changes in the GrIS topography and spatial extent.

(iii) Steps (i) and (ii) are repeated for a total of 6 iterations.

(iv) As a final step the fully coupled model (BG compset) is run for 100 years with synchronous climate–ice-sheet coupling to remove any residual inconsistencies resulting from the iterative procedure and provide a basis for assessing internal consistency and equilibration.

After 6 iterations and the final fully coupled simulation, the ice sheet model has run for a total of 9310 years ($= 6 \times 35 + 6 \times 1500 + 100$), while the ocean, land, and sea-ice components have each run for 1210 years ($= 6 \times 35 + 6 \times 150 + 100$). The atmosphere has run for 310 years ($= 6 \times 35 + 100$) — a factor of $\sim$4 less than the ocean, land and sea-ice, and a factor of $\sim$30 less than the ice sheet. As a result, the total computational cost (see Tables 1 and 2) is approximately equal to that of a 600-year simulation with the fully coupled model (1.68 M core hours / 2.8 k core hours / year $\approx$ 600 years).

4 Initial and boundary conditions

4.1 Boundary conditions

The spin-up simulation is run with a constant pre-industrial forcing protocol, consisting of observed land-ocean distribution, and 1850 CE greenhouse gas concentrations (CO_2, CH_4, N_2O, CFC11, and CFC12), orbital parameters (eccentricity, obliquity, and precession), vegetation, and land use. The relative distribution of vegetation (bare soil + 15 different vegetation types) is prescribed in each grid cell in the land model, but the ecosystem dynamics (i.e., life cycle and mortality) are prognostic. Also, land surface types (i.e., glaciated, vegetated, lakes, and urban) are dynamic to accommodate the transition between different surface conditions as the ice sheet advances and retreats (Muntjewerf, in preparation).

The topographic boundary condition in the atmosphere model is prescribed, and is read from an external file upon initialization. However, this file is updated as part of the iterative procedure, to include changes in the GrIS topography as the ice sheet evolves (see Section 3).

4.2 Initial conditions: climate

All non-ice-sheet model components were initialized from a multi-centennial, fully coupled (B compset), pre-industrial simulation with a development version of CESM2. In this prior simulation the GrIS was prescribed at its observed area and topography (Morlighem et al., 2014).

This simulation also serves as initial condition for the 1200-year fully coupled pre-industrial control simulation for CMIP6 (Danabasoglu et al., in review) (from here referred to as piControl) with prescribed GrIS geometry. We use this simulation as a benchmark for assessing viability and overall success of the iterative procedure (Section 5). Both the piControl and the present simulation adopted an identical pre-industrial forcing protocol following CMIP6 guidelines (Eyring et al., 2016).

4.3 Initial conditions: ice sheet

The ice sheet component was initialized using a protocol broadly similar to that of the CISM2 contribution to initMIP–Greenland (a model intercomparison project under CMIP6, focusing specifically on ice sheet model initialisation; Goelzer et al., 2018). The ice-sheet started from the modern observed GrIS geometry and bedrock elevation

(Morlighem et al., 2014), but with peripheral glaciers and ice caps removed. The reason is that the surface mass balance is calculated on multiple elevation classes on the nominal 1-degree land-model grid, then downscaled to the 4 km ice-sheet grid (Sellevold et al., 2019). This method works well for larger ice areas that are explicitly resolved on the coarse land-model grid. However, it becomes less accurate for smaller scale glaciers where seasonal ablation zones are poorly represented. Thus, glaciers and ice caps were removed from the initial conditions, and the model code was modified to suppress spontaneous inception outside of the contiguous ice sheet. These modifications do not however inhibit the ice sheet from expanding outside of its initial footprint due to overall mass balance and flow dynamics.

Moreover, the GrIS was initialized with an internal temperature structure corresponding to the 9 ka GrIS state (9000 years before present) in Fyke et al. (2014). This internal temperature structure was scaled via interpolation along the vertical sigma coordinates and horizontal coordinates to the observed GrIS geometry. The simulation in Fyke et al. (2014) was run over a full glacial cycle (from 130 ka to modern), using temporal variations in Greenland δ^{18}O (the ratio of heavy and light oxygen isotopes derived from Greenland ice cores) as a proxy for climate evolution. Thus, initializing the 9 ka thermal state from this prior standalone ice-sheet simulation allows for inclusion of the estimated residual thermal memory of the last glacial period, which in turn influences the final spun-up pre-industrial ice rheology at the end of the ∼9000-year simulation.

Given a constant pre-industrial forcing protocol, the ice sheet's equilibrium timescale is expected to be roughly equal to the average residence time — i.e., the amount of time an average ice parcel spends in the ice sheet before returning to the ocean via calving, runoff, or sublimation. The residence time can be estimated from the ratio of total ice sheet mass and annual average input mass flux (i.e., the GrIS-integrated surface mass balance). The modern GrIS volume is 2.93×10^{15} m^3 (Morlighem et al., 2017); hence, the ice sheet mass is roughly 2.72×10^{18} kg. High-resolution simulations with RACMO2.3 estimate the total and annually integrated GrIS surface mass balance (SMB) at approximately 350×10^{12} kg/year (Noël et al., 2018). Based on these numbers we estimate that the average residence time is around (total mass / integrated SMB ≈) 7800 years.

This calculation implicitly assumes that the ice sheet is in steady state. It also assumes a 'well-mixed' ice state, which is clearly not the case given >100 ka ice at depth (e.g. Dahl-Jensen et al., 2013). However, since the observed GrIS geometry is not actually in balance with the simulated pre-industrial climate (the steady state geometry is larger than observations; see section 5), this estimate of the residence should be viewed as a rough lower bound. Based on previous experiments, we expect that the ice sheet geometry will be in quasi-steady state in about 9000 model years (hence the 9 ka temperature structure), which is largely consistent with previous spin-up exercises with standalone ice-sheet models (e.g. Stone et al., 2010; Koenig et al., 2015).

5 Spin-up demonstration

To demonstrate the viability of the spin-up procedure, it is necessary to show that: (i) the model climate behaves predictably throughout the simulation, including the transitions between the fully coupled (BG) and data atmosphere (JG) simulation segments; (ii) the model climate — ice sheet excepted — converges toward a sufficiently similar equilibrium state as the piControl simulation with a prescribed GrIS geometry; (iii) the coupled ice-sheet component evolves differently than a standalone, uncoupled spinup simulation; and (iv) no biases in the final simulated GrIS state result from the spin-up procedure itself, as opposed to biases inherent to the CESM2 climate or CISM2 representation of ice sheet physics.

5.1 Climate: temporal evolution

Fig. 2 compares the time evolution of a selection of important ocean fields from the iterative procedure to the last 100 years of piControl. By construction, the interannual variability in the fully coupled segments (BG; gray background shading in left panels in Fig. 2) is repeated in the JG segments that follow immediately after (white background shading in left panels in Fig. 2). This is particularly reflected in the Atlantic Meridional Overturning Circulation (AMOC) strength and the surface ocean conditions, which both exhibit a pronounced year-to-year variability. In contrast, fields in the abyssal ocean are decoupled from the surface ocean on annual timescales, and therefore do not generally exhibit a similar degree of high-frequency variability.

The top panel in Figure 2 shows AMOC evolution. Overall, AMOC strength is relatively stable over the course of the simulation, though it exhibits a few episodes of both increased and decreased activity. For example, the overturning cell becomes almost 10% more vigorous in the first fully coupled segment after the model initialization, presumably because of a locally disrupted hydrological cycle in the North Atlantic due to rapid changes in the GrIS geometry (see section 5.3). This intensification is however curbed in the first JG segment, and the AMOC strength returns to a similar level as in the initial condition after ∼200 simulated ocean years. Subsequently, AMOC strength remains fairly stable, with the exception of a slight weakening after about 600 ocean model years (after the fourth fully coupled segment) and in the early stages of the extended fully coupled segment at the end of the model integration (rightmost period indicated by gray background shading in the top left panel). AMOC strength at the end of the simulation is comparable to the fully coupled spinup simulation with the B compset (cf. top right panel in Fig. 2).

The meridional heat transport (evaluated at 50°N; red contour line in Fig. 2a) is closely related to the overturning circulation, and therefore exhibits a broadly similar temporal variability as the AMOC strength. The meridional heat transport at the end of the simulation is in close agreement with that from the traditional spin-up method.

Similar to the AMOC and associated meridional heat fluxes, global average ocean temperature is comparatively stable (Fig.2b), though there is a small but systematic warming trend over the course of the simulation. The residual temperature trend in the abyssal ocean is about 0.02°C per century (approximately 0.25°C in 1210 years). This trend is consistent with the spin-up simulation with the B compset (cf. middle right panel in Fig. 2), indicating that the spin-up procedure described here is likely not responsible.

Finally, the lower panels (Fig. 2c) show the temporal evolution of global ocean salinity. Abyssal ocean salinity (red line) exhibits almost no drift over the course of the simulation. The surface salinity, on the other hand, decreases by about 0.15 PSU in the first 200 years, but then remains relatively stable.

5.2 Climate: equilibrium state

Figure 3 compares 100-year annual climatologies derived from the end of the iterative simulation with the end of the piControl spinup simulation (B compset with a prescribed GrIS geometry). It is apparent that both simulations are converging toward the same overall climatological state, with the exception of an appreciable cold anomaly over Greenland and the northern North Atlantic in the iterative simulation. The cool temperatures over the ice sheet are a direct result of the elevation feedback, as both the GrIS height and morphology are different in the two simulations (elevation differences of several 100 meters are simulated over the central parts of the ice sheet; see Section 5.4). Cold air developed over the GrIS interior is then likely advected out over the surrounding ocean by mean simulated atmospheric flow. In addition, the coupled GrIS interacts directly (and more realistically) with the ocean through runoff fluxes and solid ice discharge (calv-

ing) in marine terminating outlet glaciers. The larger ice sheet at the end of the iterative procedure results in overall increased freshwater fluxes relative to piControl (the average surface mass balance has increased by around 100 Gt/year compared to the initial state; see Fig. 4 and Table 3).

Cooler sea-surface temperatures resulting from GrIS coupling also likely helps amplify the density-driven deep convection in the North Atlantic, leading to a strengthening (though, generally only a few percent) of the North Atlantic deep water branch of the meridional overturning circulation (Fig. 3b,d), relative to the piControl with a prescribed ice sheet.

The difference plot of surface temperature (Fig. 3c) also reveals (statistically significant) warm anomalies scattered across land areas in the tropics. The origin of these warm anomalies remains elusive, but, owing to their patchy appearance, we speculate that they are due to local inconsistencies in the vegetation cover between the two simulations. The vegetation distribution and phenology is prescribed in each grid cell, but the life cycle is determined in part by the local temperature, precipitation, and soil nutrients that vary transiently over the course of the simulation. The location and intensity of precipitation in the intertropical convergence zone is slightly modulated relative to piControl, which results in slight seasonal variations in gross primary production (not shown). This is at least partially explained by the North Atlantic cold anomaly, and is likely not an artifact of our methodological design.

5.3 Ice sheet: temporal evolution

Temporal GrIS geometry and mass balance evolution is shown in Fig. 4. The global pre-industrial climate simulated by CESM2 qualitatively reproduces the spatial pattern of observed surface mass balance remarkably well. (Snapshots of the equilibrium ice sheets are shown in Fig. 5 and are discussed further below). However, net positive precipitation biases in the ice-sheet interior and over peripheral tundra render the equilibrium GrIS substantially larger than modern observations, as ice mass accumulates during the multi-millennial spin-up simulation (Table 3).

As shown in Fig. 4 and Table 3, the ice sheet grows piecemeal, with rapid bursts just after initialization (BG1) and after about 2000 model years, followed by more quiescent periods with comparatively smaller changes in the overall ice-sheet geometry. The largest single area expansion occurs around model year 2000, as the ice sheet dynamically expands into the tundra of Peary Land and Crown Prince Christian Land in the far north (see Fig. 5). However, these regions have little precipitation, and the new ice is therefore thin and not reflected in a corresponding abrupt increase in the overall ice-sheet volume (Fig. 4b and Table 3).

The ice-sheet area also increases rapidly in the first few decades of the simulation (most easily seen in Table 3). This expansion is partly explained by a mass imbalance prompted by the CISM2 initial conditions. Both the calving flux and basal mass balance are initially small, while the surface mass balance, which is calculated in the land model, is already more or less spun up (see Fig. 4c and Table 3). The initial surface mass balance is 490±65 Gt/year, which is considerably higher than the modern (1960-1990 CE) estimate of about 350 Gt/year from the regional climate model RACMO2.3 (Noël et al., 2018). The SMB increases in the first half of the simulation, and stabilizes at around 600 Gt/year after approximately 5000 model years (Table 3). This increase is largely a function of positive feedbacks between ice sheet area and SMB: as the area grows, the accumulation area and also the accumulation to ablation area ratio (accumulation/ablation) grows, promoting further growth.

The initial mass imbalance corresponds to a global mean sea-level decrease of about 1.3 mm/year. In comparison, the residual drift at the end of the simulation (end of BG7)

is 0.03±0.23 mm/year. Interannual variability in (total) mass balance is dominated by the surface mass balance term (Table 3), while the other components — calving flux and basal mass balance — account for much less variability: the mass balance at the end of the simulation is -9±83 Gt/year, with contributions from surface mass balance 591±83 Gt/year, basal mass balance -24±0.08 Gt/year, and calving fluxes 577±4 Gt/year (see Table 3).

5.4 Ice sheet: spatial fields

The final spun-up GrIS area is almost 15% larger than modern observations (Table 3). Much of this difference comes from the glaciation of peripheral tundra that is ice-free in the modern climate. In this final state, ice everywhere reaches the sea, with the notable exception of Washington Land in the far north, and much of the southwestern margin that, in broad agreement with observations, remains far inland (Fig. 5a-c). Consequently, ice volume is also overestimated, with considerable thickness anomalies in both the north-central interior and the southwestern parts of the ice sheet. These elevation differences are primarily attributed to positive precipitation anomalies (mostly in the form of snowfall) over the majority of the ice-sheet interior. Conversely, anomalously low precipitation leaves the ice thickness underestimated along the northern/northwestern margins. The total ice volume is approximately 8.3 m sea-level equivalent, which exceeds modern estimates of around 7.4 m sea-level equivalent (Morlighem et al., 2017) by around 12%. While this bias is significant, we note that 1) it is similar in sign to many other simulations of GrIS state using spin-up (versus initialization) approaches; and 2) the bias is not a result of the spin-up procedure itself, but rather reflects intrinsic climate and ice sheet model behaviour.

In broad agreement with previous studies (e.g. van Kampenhout et al., 2019), the model does a good job representing the overall spatial SMB patterns, but struggles to capture the local spatial gradients. Precipitation is typically underestimated on the ice-sheet periphery and overestimated in the interior. This is at least partly understood from the coarse grid resolution in the atmosphere model, which is unable to properly capture the steep ice-sheet margins, and thus underestimates orographic precipitation in coastal areas and along the ice-sheet edges (van Kampenhout et al., 2019). The extent and magnitude of the observed ablation areas are well represented along the western margin. However, positive SMB biases are present in the far north and along the eastern margin where the ice sheet has expanded well outside of its modern observed footprint. These regions are tundra fields in the modern climate, and the SMB should therefore be effectively calculated as zero.

Despite SMB biases, there is generally good spatial agreement between the simulated and the observed velocity fields (Joughin et al., 2010), although simulated outlet glaciers are more numerous than in reality because of a larger fraction of the ice margin is marine-terminating. The highest velocities in the major ice streams tend to be underestimated (Fig. 5) — the highest simulated surface velocity is 6 km/year, which is substantially lower than the 10 km/year that are regularly observed in Jakobshavn Isbræ (e.g., Joughin et al., 2004; Rignot & Mouginot, 2012). Moreover, the ice streams in the northwest are narrower, extend farther inland, and are more well defined compared to observations. The Northeast Greenland Ice Stream is however more diffuse and does not extend as far inland as observed, which is consistent with the standalone ice-sheet model simulations in Lipscomb et al. (2019). The model also simulates internal multi-millennial oscillations of the Northeast Greenland Ice Stream and the Humboldt glacier (S. Bradley, personal communication), resulting in horizontal ice stream migrations, which may help explain regional differences from observations which — to the extent this oscillation is realistic — likely only capture one phase of the long-term variability.

The ice-sheet's internal temperature structure plays a role in regulating ice rheology and internal flow dynamics. Figure 6 plots a vertical temperature cross section through

the summit location of the equilibrium ice sheet. The temperature profile at Summit closely matches the in-situ temperature profile from the GRIP core (Dahl-Jensen et al., 1998) (cf. blue and black lines in Fig. 6b). Although most of the thermal memory of the initial condition has vanished after 9000 model years (cf. red and blue lines in Fig. 6b), the vertical temperature profile retains a weak thermal signature of the Last Glacial Period. This is manifested as a sub-surface cold anomaly in the interior of the ice sheet (Fig. 6a), which reflects recent emergence from the Last Glacial Period; see further discussion in Fyke et al. (2014).

5.4.1 Ice sheet: comparison with ice-sheet-only simulations

The simulations discussed so far have a time-varying, two-way interactive climate–ice-sheet coupling. It is important to understand how much these boundary conditions affect the equilibrium ice sheet. To do this, we conducted a set of ice-sheet-only simulations (T compset; section 2.1.3) with a time-invariant SMB forcing (Lipscomb et al., 2013; Sellevold et al., 2019). These experiments were branched from the fully coupled segments of the iterative procedure (using 30 consecutive years of SMB forcing from the branch point), and were run for lengths corresponding to the end of the main spinup simulation. Elevation feedbacks are implicitly accounted for when downscaling the SMB forcing to the CISM2 grid in these ice-sheet-only simulations. Nevertheless, comparisons with the iterative simulation provides a qualitative assessment of how the equilibrium state is influenced by interactive climate–ice-sheet coupling.

Results are shown in Fig. 4 and Table 4. The GrIS geometry evolves in a broadly similar fashion in both experiments (cf. colored lines in Fig. 4). However, ice-sheet-only simulations consistently underestimate the GrIS area and volume from the main experiment, indicating that interactive climate–ice-sheet coupling favours growth (Fig. 4a,b and Table 4). Since the general climate forcing itself favors growth, this suggests that the net sum of ice-sheet/Earth system feedbacks as represented in the simulation is positive.

The importance of two-way interactive climate–ice-sheet coupling is even more apparent in Fig. 7, which compares the thickness and vertical temperature structure between the ice sheet from the end of the iterative procedure and the ice-sheet-only simulations. The first ice-sheet-only simulation (T1), which is using SMB forcing from the first fully coupled simulation (BG1), converges toward a state with substantial elevation differences (of order 100 meters) over almost the entire domain. The internal temperature distribution is generally biased warm, which is consistent with a surface temperature forcing that is based on a considerably lower ice-sheet topography than the fully-coupled equilibrium state.

Differences between standalone and coupled simulations become progressively smaller for ice-sheet-only simulations branched from the main experiment at later points, and ice-sheet-only simulations started after year 5000 are almost indistinguishable from the main experiment. However, similarities in ice-sheet geometry and internal temperature between the iterative spinup simulation and the ice-sheet-only simulations belie the fact that the ice sheet is not actually in equilibrium after 9000 model years. The ice sheet thickness and internal temperature diverge significantly when running out the ice-sheet-only simulations for an additional 10 kyrs beyond the end of the iterative procedure (Fig. 7g,h) — a similar divergence is obtained from all ice-sheet-only simulations when extended out far beyond the end of the iterative procedure. It is thus not apparent that the iterative procedure could have been terminated prematurely (e.g. after BG5) and replaced with the more computationally efficient ice-sheet-only configuration.

6 Summary and discussion

In this work we have described and demonstrated a computationally tractable, iterative procedure for spinning up a comprehensive Earth system model. The utility of the method is illustrated by spinning up a CESM2 (Danabasoglu et al., in review) pre-industrial climate, using a model configuration that includes an interactive Greenland Ice Sheet. Beyond this specific application, which we deem critical to the practical use of coupled ice sheet/Earth system models, we emphasize that the methods described here are potentially general in nature, and therefore may also apply to other ESM configurations. For example, these methods may be a viable alternative for spinning up the deep ocean circulation in a coupled model setting, and it may also be applicable for spinning up ESM climate for certain paleo-climate applications.

The model climate is spun up by alternating between a fully coupled model configuration, and an equivalent configuration where the atmospheric component is substituted by a prescribed data model. In order to converge to the results of an equivalent free-running fully coupled model integration, simulation segments with the data atmosphere are kept short enough to prevent unrealistic climate drift, yet sufficiently long to capitalize on the greater throughput and lower computational cost relative to the fully coupled configuration; see Tables 1 and 2. With this approach, the cost of the atmospheric model (which accounts for almost 70% of the total cost of CESM2) is greatly reduced, with no significant divergence of final spin-up state.

We estimate that the computational requirements for the iterative procedure are more than an order of magnitude smaller than for an equivalent application with a fully coupled model. It is also around 30% lower than a traditional asynchronous climate–ice-sheet coupling commonly adopted for long integrations with climate–ice-sheet models (e.g. Ridley et al., 2005); see Table 2. Our analysis of computational savings is based on an iterative approach that involves 35 years of coupled model simulation, followed by 150 years of simulation with the data atmosphere configuration. We determined that this comprises a reasonable balance between resource savings and accurate reproduction of an acceptable final, fully coupled and internally consistent climate state. Nonetheless, further cost savings could likely be obtained with adjustments to the calibration procedure.

In a recent study, Ziemen et al. (2019) introduced a novel acceleration technique for running ECHAM5 with interactive ice sheets over glacial timescales. Similar to our methodology, they adopted a periodic synchronous coupling and achieved substantial computational savings by recycling atmospheric data over large parts of the simulation. Their implementation is however notably different from ours, which makes for an interesting comparison with our methodological design.

Ziemen et al. (2019) effectively implemented a 1:10:100 atmosphere–climate–ice-sheet coupling, where the fully coupled model was run for a single year every 10 ocean–land–sea-ice model years, and every 100 ice-sheet model years. Between these segments, the data atmosphere provided atmospheric forcing stored from the previous five fully coupled model years. This means that the first and last years of the atmospheric forcing data are temporally separated by as much as 50 years. This modeling approach was designed specifically to reduce overall computational expenses. However, similar to all accelerated modeling implementations, it could potentially introduce inconsistencies that may influence the overall climate evolution.

For example, several of the major modes of variability (e.g., ENSO & NAO) typically occur with a periodicity of seasonal/interannual to sub-decadal timescales. Hence, sampling every 10 model years could potentially result in an aliased frequency of major climate modes in the atmosphere data archive. Moreover, only running the fully coupled model for a single year after advancing the overall climate/ice-sheet state by 10/100

years could possibly introduce inconsistencies in the long-term climate evolution. Specifically, although the atmosphere is quick to adapt to changes in the planetary boundary conditions, it still can take several months for the atmosphere to fully forget abrupt changes in surface conditions (notably the ice sheet topography).

The philosophy adopted when designing our simulation procedure was to: (1) capture the model's internal climate variability by prescribing high-frequency atmospheric data over a standard climatological period of three decades; (2) update this data archive (hence regain internal consistency) with reasonable periodicity by running comparatively short segments with the data atmosphere; and (3) suppress "shocks" in the climate system when transitioning between the fully coupled and data atmosphere configurations. The latter was achieved by running the fully coupled model for five years before saving data to the forcing archive. Hence, the atmosphere is given sufficient time to adjust to changes in the surface climate state and the GrIS topography, which in principle reduces spurious climate drift in the segments with the data atmosphere.

It is possible that none of these concerns are major issues for the interesting and pioneering simulations described in Ziemen et al. (2019), and we concede that some of the techniques we have implemented may not be strictly necessary for the goal of generating a climate/ice-sheet state that is close to that obtained from a fully coupled model with a synchronous climate/ice-sheet coupling. Nevertheless, we advice general caution when applying asynchronous simulation techniques, because there is significant risk of inadvertently introducing unwanted model behavior.

Conversely, we highlight that the simulations we described here have their own set of shortcomings. Most prominently, the equilibrium ice sheet is 10 to 20% larger than modern observations. However, this is primarily a result of biases in the simulated GrIS mass balance, and not a product of the spin-up procedure itself. Notably, van Kampenhout et al. (2019) recently showed that the relatively coarse (nominal 1°) horizontal resolution of the atmosphere model can help explain biases in the surface mass balance. They further showed that local grid refinement over the ice sheet improves simulation of precipitation gradients on the ice sheet edges, and also reduces excessive moisture intrusion into the ice sheet interior. Simulations with variable resolution grids will likely be more commonplace in the future, and should be entirely compatible with spin-up approaches such as described here.

The final coupled GrIS and Earth system state achieved via the spin-up technique presented here can be put in context with other results from the Ice Sheet Model Intercomparison Project for CMIP6 (ISMIP6; Nowicki et al., 2016) and its initMIP-Greenland component (Goelzer et al., 2018). Unlike many intercomparison projects, initMIP-Greenland puts few constraints on how participating models implement SMB forcing, numerical methods, model parameter choices, ice flow approximations, etc. Of the 35 standalone ice sheet simulations submitted by 17 participating groups, 22 simulations used a similar initialization technique that, like ours, is based on a freely evolving ice sheet, while the remaining used data assimilation of surface topography and/or surface velocities. All the freely evolving initMIP-Greenland simulations overestimated both ice sheet volume (ranging from 2.98 to 3.41 M km^3, compared to the actual 2.95 M km^3 volume (Morlighem et al., 2014)), and ice sheet area (ranging from 1.66 to 2.10 M km^2, compared to the observed 1.65 M km^2). Of these 22 simulations, five ended with a larger volume than from our iterative procedure (ranging from 0.05 to 0.20 M km^3 larger), and five simulations ended with a larger GrIS area (differences up to 0.10 M km^2). Similar to our final ice sheet state, eight of the 22 freely evolving simulations showed partial or full glaciation of the Northern tundra. An additional four simulations overestimated the glaciated area of the Flade Isblink ice cap in far northeastern Greenland; in two cases this ice area is connected to the main ice sheet. This comparison is however not entirely fair, as several of these models used a constant (not modulated by GrIS geometry changes) SMB forcing from high-resolution regional climate models constrained by reanalysis data when spinning up their

ice sheet models. Regional climate models can better represent topography and local SMB gradients than comparatively coarser resolution ESMs, thus resulting in an overall more realistic GrIS state.

In previous work with one-way-coupled CESM1-CISM1 (Lipscomb et al., 2013), GrIS initialization was carried out with an ensemble of 100 ice-sheet-only simulations via Latin Hypercube Sampling of key ice sheet model parameters (similar to Stone et al., 2010). These spin-ups were forced with the climate from a single fully coupled CESM1 simulation. In all ensemble members the resulting total ice sheet volume and area were overestimated compared with observations. Compared with the iterative procedure, the ice volumes were mainly larger (difference ranging from -0.05 to +0.65 $\mathrm{M\,km^3}$) while the GrIS areas were smaller (-0.03 $\mathrm{M\,km^2}$ in all simulations), with most of the excess volumes added to the northern and southern margins, similar to the present case.

Earlier work on coupled climate/ice sheet modeling spun up the ice sheet through the two glacial cycles using perturbed precipitation and temperature fields (Ridley et al., 2005). These coupled simulations also overestimated the ice sheet volume compared to the present-day observed GrIS, though 0.25 $\mathrm{M\,km^3}$ smaller than the results presented here, mainly because the SMB was much lower (285 Gt/year versus 591 Gt/year). Moreover, Vizcaino et al. (2015) utilized a two-step spin-up procedure, where the ice sheet was initially forced with uncorrected precipitation and temperature fields until 9 ka, and from then bidirectionally coupled to a climate model with an energy-balance-based SMB calculation. This produced an initial GrIS that exceeded the observed present-day ice sheet in both area and volume, though with respect to the current study the area was 0.05 $\mathrm{M\,km^2}$ smaller and the volume was 0.11 $\mathrm{M\,km^3}$ smaller. Altogether, the spun-up GrIS state from our iterative procedure is well within the range of previous ice sheet model spin-up results.

7 Conclusions

In this work we have described and demonstrated a computationally efficient iterative procedure for spinning up coupled climate–ice sheet models. We demonstrated its applicability by spinning up the pre-industrial climate in CESM2, with a two-way interactive ice-sheet model over Greenland (CISM2). We summarize our conclusions as follows:

(i) The iterative spinup procedure alternates between a fully coupled (BG compset) and a computationally cheaper configuration (JG compset) where the atmospheric component is replaced by a data model. By periodically regenerating the atmospheric forcing, the data atmosphere remains adequately constrained, thus ensuring that the broader coupled model state also does not drift unrealistically.

(ii) The simulated climate at the end of the spin-up procedure is similar to the pre-industrial control climate from a 1200-year fully coupled spinup simulation, indicating that the climate in our iterative procedure converges towards a climate state that is consistent with the state achieved using a traditional spin-up approach without interactive ice sheets.

(iii) The iterative method is an order of magnitude faster and cheaper than a "brute force" spinup method, and also significantly faster and cheaper than other accelerated/asynchronous spinup methods.

(iv) We suggest that the iterative method presented here can provide a faster and cheaper method for spinning up computationally expensive fully coupled climate and Earth-system models, with or without interactive ice sheet components.

Finally, we highlight that the pre-industrial climate/ice-sheet state achieved via the methodologies described in this manuscript will serve as key initial conditions for tran-

sient simulations with CESM2/CISM2 in support of ISMIP6 fully-coupled historical and future simulations. The results presented in future ISMIP6 and CMIP6 studies with an interactive GrIS thus will rely substantially on the techniques developed and presented in the current study.

8 Code Availability

CESM2 is open source software, freely available at: http://www.cesm.ucar.edu/.

Acknowledgments

The CESM project is supported primarily by the National Science Foundation. This material is based upon work supported by the National Center for Atmospheric Research, which is a major facility sponsored by the National Science Foundation under Cooperative Agreement No. 1852977. Computing and data storage resources, including the Cheyenne supercomputer (doi:10.5065/D6RX99HX), were provided by the Computational and Information Systems Laboratory (CISL) at NCAR. The authors also wish to thank colleagues at NCAR for invaluable assistance with the experiment design: Jim Edwards and Gary Strand for improving model performance and data archiving, Keith Lindsay and Mariana Vertenstein for scripting and streamlining the workflow, and Peter Lauritzen and Julio Bacmeister for providing the CAM topography scripts and for help integrating these tools into our workflow. The topography updating routines rely on the GMTED2010 topography dataset, which is curated and made publicly available by the United States Geological Survey (USGS). LM, MV and SLB acknowledge funding from the European Research Council (grant no. ERC-StG-678145-CoupledIceClim). Data presented in this work is publicly available on Earth System Grid (https://www.earthsystemgrid.org/).

References

Alexander, K., & Easterbrook, S. M. (2015). The software architecture of climate models: a graphical comparison of cmip5 and emicar5 configurations. *Geoscientific Model Development*, *8*(4), 1221–1232. doi: 10.5194/gmd-8-1221-2015

Aschwanden, A., Fahnestock, M. A., & Truffer, M. (2016). Complex greenland outlet glacier flow captured. *Nature communications*, *7*, 10524.

Beljaars, A., Brown, A. R., & Wood, N. (2004). A new parametrization of turbulent orographic form drag. *Quarterly Journal of the Royal Meteorological Society*, *130*(599), 1327–1347.

Dahl-Jensen, D., Albert, M. R., Aldahan, A., Azuma, N., Balslev-Clausen, D., Baumgartner, M., ... Zheng, J. (2013). Eemian interglacial reconstructed from a Greenland folded ice core. *Nature*, *493*(7433), 489.

Dahl-Jensen, D., Mosegaard, K., Gundestrup, N., Clow, G. D., Johnsen, S. J., Hansen, A. W., & Balling, N. (1998). Past temperatures directly from the greenland ice sheet. *Science*, *282*(5387), 268–271.

Danabasoglu, G., Lamarque, J.-F., Bacmeister, J., Bailey, D. A., DuVivier, A. K., Edwards, J., ... Strand, W. G. (in review). The Community Earth System Model version 2 (CESM2). *J. Adv. Model. Earth Syst.*.

Danielson, J. J., & Gesch, D. B. (2011). *Global multi-resolution terrain elevation data 2010 (gmted2010)* (Open File Rep. No. 2011-1073). US Geological Survey. doi: https://doi.org/10.3133/ofr20111073

DeConto, R., Pollard, D., & Harwood, D. (2007). Sea ice feedback and Cenozoic evolution of Antarctic climate and ice sheets. *Paleoceanography*, *22*, PA3214. doi: 10.1029/2006PA001350

Eyring, V., Bony, S., Meehl, G. A., Senior, C. A., Stevens, B., Stouffer, R. J., & Taylor, K. E. (2016). Overview of the Coupled Model Intercomparison Project Phase 6 (CMIP6) experimental design and organization. *Geoscientific Model*

Development, *9*(LLNL-JRNL-736881), 1937–1958.

Fretwell, P., Pritchard, H. D., Vaughan, D. G., Bamber, J., Barrand, N., Bell, R., ... Zirizzotti, A. (2013). Bedmap2: improved ice bed, surface and thickness datasets for antarctica. *The Cryosphere*, *7*, 375–393. doi: http://dx.doi.org/10.5194/tc-7-375-2013

Fyke, J. G., Sacks, W. J., & Lipscomb, W. H. (2014). A technique for generating consistent ice sheet initial conditions for coupled ice sheet/climate models. *Geoscientific Model Development*, *7*(3), 1183–1195. Retrieved from `http://www.geosci-model-dev.net/7/1183/2014/` doi: 10.5194/gmd-7-1183-2014

Fyke, J. G., Sergienko, O., Lofverstrom, M., Price, S., & Lenaerts, J. T. (2018). An overview of interactions and feedbacks between ice sheets and the earth system. *Reviews of Geophysics*. doi: 10.1029/2018RG000600

Ganopolski, A., R, C., & Claussen, M. (2010, 04). Simulation of the last glacial cycle with a coupled climate ice-sheet model of intermediate complexity. *Climate of the Past*, *5*. doi: 10.5194/cpd-5-2269-2009

Goelzer, H., Nowicki, S., Edwards, T., Beckley, M., Abe-Ouchi, A., Aschwanden, A., ... Ziemen, F. A. (2018). Design and results of the ice sheet model initialisation experiments initmip-greenland: an ismip6 intercomparison. *The Cryosphere*, *12*(4), 1433–1460. Retrieved from `https://www.the-cryosphere.net/12/1433/2018/` doi: 10.5194/tc-12-1433-2018

Goldberg, D. N. (2011). A variationally derived, depth-integrated approximation to a higher-order glaciological flow model. *J. Glaciol.*, *57*(201), 157-170. doi: 10.3189/002214311795306763

Graversen, R. G., Mauritsen, T., Tjernström, M., Källén, E., & Svensson, G. (2008). Vertical structure of recent arctic warming. *Nature*, *451*(7174), 53.

Griffies, S. M., Biastoch, A., Böning, C., Bryan, F., Danabasoglu, G., Chassignet, E. P., ... Yin, J. (2009). Coordinated ocean-ice reference experiments (cores). *Ocean modelling*, *26*(1-2), 1–46.

Griffies, S. M., Danabasoglu, G., Durack, P. J., Adcroft, A. J., Balaji, V., Böning, C. W., ... Yeager, S. G. (2016). Omip contribution to cmip6: experimental and diagnostic protocol for the physical component of the ocean model intercomparison project. *Geoscientific Model Development*, *9*(9), 3231–3296. Retrieved from `https://www.geosci-model-dev.net/9/3231/2016/` doi: 10.5194/gmd-9-3231-2016

Ilyina, T., Six, K. D., Segschneider, J., Maier-Reimer, E., Li, H., & Núñez-Riboni, I. (2013). Global ocean biogeochemistry model hamocc: Model architecture and performance as component of the mpi-earth system model in different cmip5 experimental realizations. *Journal of Advances in Modeling Earth Systems*, *5*(2), 287–315.

Joughin, I., Abdalati, W., & Fahnestock, M. (2004). Large fluctuations in speed on Greenland's Jakobshavn Isbrae glacier. *Nature*, *432*(7017), 608–610. doi: 10.1038/nature03130

Joughin, I., Smith, B. E., Howat, I. M., Scambos, T., & Moon, T. (2010). Greenland flow variability from ice-sheet-wide velocity mapping. *Journal of Glaciology*, *56*(197), 415–430.

Koenig, S., Dolan, A., De Boer, B., Stone, E., Hill, D., DeConto, R., ... others (2015). Ice sheet model dependency of the simulated Greenland Ice Sheet in the mid-Pliocene. *Climate of the Past*, *11*(3), 369–381.

Lauritzen, P. H., Bacmeister, J. T., P., C., & Taylor, M. A. (2015). Ncar global model topography generation software for unstructured grids. *Geosci. Model Dev.*, *8*, 3975-3986. doi: 10.5194/gmd-8-3975-2015

Lawrence, D., Fisher, R., Koven, C., Oleson, K., Swenson, S., Bonan, G., ... Zeng, X. (2019). The community land model version 5: Description of new features, benchmarking, and impact of forcing uncertainty. *Submitted to J. Adv. Model. Earth Syst.*.

Leguy, G., Lipscomb, W., & Sacks, W. (2019). *Cesm land ice documentation and user guide* (Tech. Rep.). National Center for Atmospheric Research. Retrieved from `https://escomp.github.io/cism-docs/cism-in-cesm/versions/release-cesm2.0/html/index.html` (Last accessed 20 October 2019)

Lipscomb, W., Fyke, J., Vizcaíno, M., Sacks, W., Wolfe, J., Vertenstein, M., ... Lawrence, D. (2013). Implementation and initial evaluation of the Glimmer Community Ice Sheet Model in the Community Earth System Model. *Journal of Climate*, *26*, 7352–7371. doi: 10.1175/JCLI-D-12-00557.1

Lipscomb, W., Price, S., Hoffman, M., Leguy, G., Bennett, A., Bradley, S., ... Worley, P. (2019). Description and evaluation of the community ice sheet model (cism) v2.1. *Geosci. Model Dev.*, *12*, 387-424. doi: https://doi.org/10.5194/gmd-12-387-2019

Lofverstrom, M., & Liakka, J. (2016). On the limited ice intrusion in Alaska at the LGM. *Geophysical Research Letters*, *43*, 11,030–11,038. doi: 10.1002/2016GL071012

Lofverstrom, M., Liakka, J., & Kleman, J. (2015). The North American Cordillera—An impediment to growing the continent-wide Laurentide Ice Sheet. *Journal of Climate*, *28*(3), 9433–9450.

Morlighem, M., Rignot, E., Mouginot, J., Seroussi, H., & E., L. (2014). Deeply incised submarine glacial valleys beneath the greenland ice sheet. *Nature Geoscience*, *7*, 418–422. doi: 10.1038/ngeo2167,http://www.nature.com/ngeo/journal/vaop/ncurrent/full/ngeo2167.html

Morlighem, M., Williams, C. N., Rignot, E., An, L., Arndt, J. E., Bamber, J. L., ... Zinglersen, K. B. (2017). BedMachine v3: Complete bed topography and ocean bathymetry mapping of Greenland from multibeam echo sounding combined with mass conservation. *Geophysical Research Letters*, *44*(21), 11–051. doi: 10.1002/2017GL074954

Muntjewerf, e. a., L. (in preparation). Ice-sheet/climate coupling between cesm2.1 and cism2.1. *Journal of Advances in Modeling Earth Systems*.

Noël, B., Van De Berg, W., Van Meijgaard, E., Kuipers Munneke, P., Van De Wal, R., & Van Den Broeke, M. (2015). Evaluation of the updated regional climate model racmo2. 3: summer snowfall impact on the greenland ice sheet. *The Cryosphere*, *9*(5), 1831–1844.

Noël, B., van de Berg, W. J., Wessem, V., Melchior, J., Van Meijgaard, E., Van As, D., ... others (2018). Modelling the climate and surface mass balance of polar ice sheets using racmo2-part 1: Greenland (1958-2016). *Cryosphere*, *12*(3), 811–831.

Nowicki, S. M. J., Payne, A., Larour, E., Seroussi, H., Goelzer, H., Lipscomb, W., ... Shepherd, A. (2016). Ice sheet model intercomparison project (ismip6) contribution to cmip6. *Geoscientific Model Development*, *9*(12), 4521–4545. Retrieved from `https://www.geosci-model-dev.net/9/4521/2016/` doi: 10.5194/gmd-9-4521-2016

Ridley, J., Huybrechts, P., Gregory, J., & Lowe, J. (2005). Elimination of the Greenland ice sheet in a high CO_2 climate. *Journal of Climate*, *18*, 3409–3427. doi: 10.1175/JCLI3482.1

Rignot, E., & Kanagaratnam, P. (2006). Changes in the velocity structure of the greenland ice sheet. *Science*, *311*(5763), 986–990.

Rignot, E., & Mouginot, J. (2012). Ice flow in Greenland for the international polar year 2008–2009. *Geophysical Research Letters*, *39*(11).

Rignot, E., Mouginot, J., Scheuchl, B., van den Broeke, M., van Wessem, M. J., & Morlighem, M. (2019). Four decades of antarctic ice sheet mass balance from 1979–2017. *Proceedings of the National Academy of Sciences*, *116*(4), 1095–1103.

Rutt, I., Hagdorn, M., Hulton, N., & Payne, A. (2009). The Glimmer community ice sheet model. *J. Geophys. Res.*, *114*, F02004.

Sellevold, R., van Kampenhout, L., Lenaerts, J. T. M., Noël, B., Lipscomb, W. H., & Vizcaino, M. (2019). Surface mass balance downscaling through elevation classes in an Earth system model: application to the Greenland ice sheet. *The Cryosphere*(13), 3193–3208. doi: 10.5194/tc-13-3193-2019

Serreze, M. C., & Francis, J. A. (2006). The arctic amplification debate. *Climatic change*, *76*(3-4), 241–264.

Smith, Jones, P., Briegleb, B., Bryan, F., Danabasoglu, G., Dennis, J., ... Yeager, S. (2010). The parallel ocean program (POP) reference manual. *Los Alamos National Lab Technical Report*, *141*.

Smith, D. M., Screen, J. A., Deser, C., Cohen, J., Fyfe, J. C., García-Serrano, J., ... Zhang, X. (2019). The polar amplification model intercomparison project (pamip) contribution to cmip6: investigating the causes and consequences of polar amplification. *Geoscientific Model Development*, *12*(3), 1139–1164.

Stone, E., Lunt, D., Rutt, I., & Hanna, E. (2010). Investigating the sensitivity of numerical model simulations of the modern state of the Greenland ice-sheet and its future response to climate change. *The Cryosphere*, *4*(3), 397–417.

Tesfa, T. K., Li, H.-Y., Leung, L., Huang, M., Ke, Y., Sun, Y., & Liu, Y. (2014). A subbasin-based framework to represent land surface processes in an earth system model. *Geoscientific Model Development*, *7*(3), 947–963.

Thornton, P. E., & Rosenbloom, N. A. (2005). Ecosystem model spin-up: Estimating steady state conditions in a coupled terrestrial carbon and nitrogen cycle model. *Ecological Modelling*, *189*(1-2), 25–48.

Van den Broeke, M. R., Enderlin, E. M., Howat, I. M., Kuipers Munneke, P., Noël, B. P., Jan Van De Berg, W., ... Wouters, B. (2016). On the recent contribution of the greenland ice sheet to sea level change. *The Cryosphere*, *10*(5), 1933–1946.

van Kampenhout, L., Lenaerts, J. T., Lipscomb, W. H., Sacks, W. J., Lawrence, D. M., Slater, A. G., & van den Broeke, M. R. (2017). Improving the representation of polar snow and firn in the Community Earth System Model. *Journal of Advances in Modeling Earth Systems*, *9*(7), 2583–2600.

van Kampenhout, L., Rhoades, A., Herrington, A., Zarzycki, C., Lenaerts, J., Sacks, W., & Van Den Broeke, M. (2019). Regional grid refinement in an earth system model: impacts on the simulated greenland surface mass balance. *Cryosphere*, *13*(6), 1547–1564.

Vizcaino, M., Mikolajewicz, U., Ziemen, F., Rodehacke, C. B., Greve, R., & Van Den Broeke, M. R. (2015). Coupled simulations of greenland ice sheet and climate change up to ad 2300. *Geophysical Research Letters*, *42*(10), 3927–3935.

Ziemen, F., Kapsch, M.-L., Klockmann, M., & Mikolajewicz, U. (2019). Heinrich events show two-stage climate response in transient glacial simulations. *Climate of the Past*, *15*, 153–168.

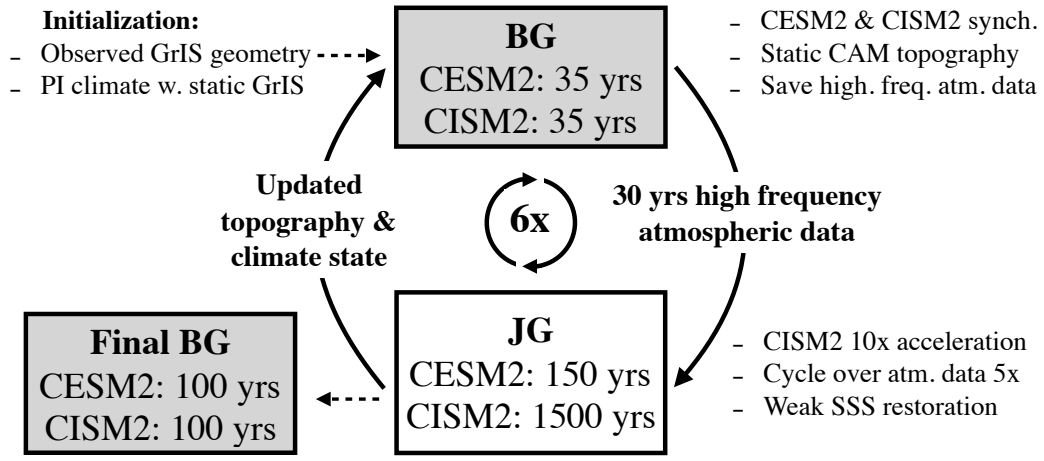

Figure 1. Schematics illustration of iterative spinup procedure. The fully coupled simulations (BG compset) were run for 35 years with a synchronous climate–ice-sheet coupling. High-frequency atmospheric fluxes were extracted from the last 30 years. Subsequently, the coupled model with a data atmosphere (JG compset) was run for 150 years with a 10x acceleration of the ice sheet component (1500 ice-sheet years), looping 5 times over the atmospheric data archive. The CAM topography was updated before a new fully coupled simulation was run, thus starting the cycle over. A total of 6 iterations were run, followed by a 100 year long fully coupled simulation to remove inconsistencies from the iterative procedure. This resulted in 9310 CISM2 years and 1210 simulated years with the ocean, sea-ice, and land models.

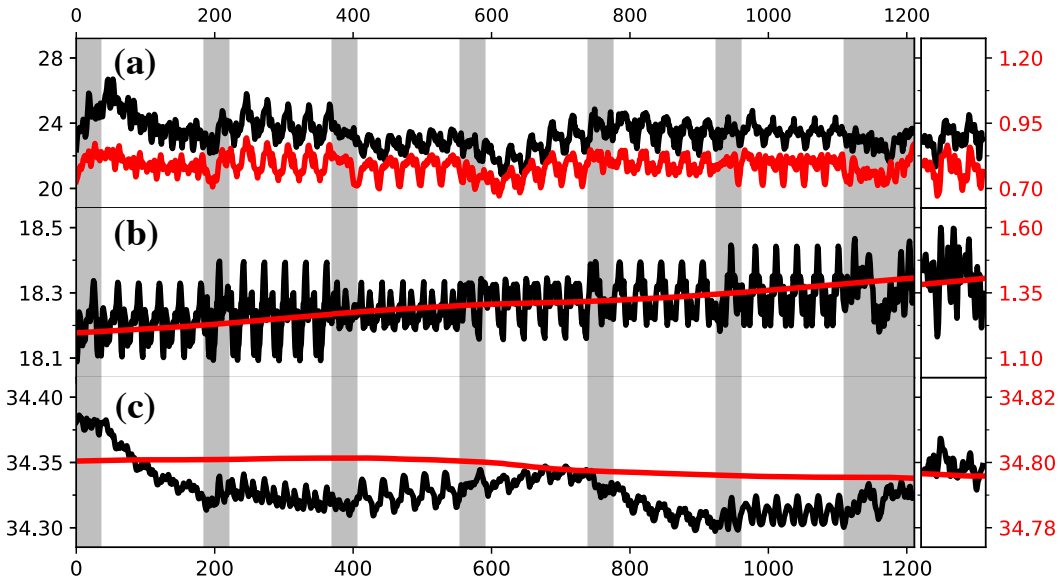

Figure 2. Annual mean timeseries comparing the iterative spinup procedure (left) with 100 years of the piControl simulation with prescribed GrIS geometry (right). (a) Atlantic meridional overturning circulation (AMOC) [Sv] (maximum meridional overturning streamfunction below 500 m and north of 28°S; black), and northward heat transport at 50°N [PW] (red); (b) global mean sea-surface temperature [°C] (black), and abyssal ocean [°C] (red); (c) global mean sea-surface salinity [PSU] (black), and abyssal ocean [PSU] (red). Fully coupled (BG compset) segments are indicated by gray background in the left panels; JG compset was used elsewhere.

Table 1. Comparison of number of: core-hours per simulated year (cost), simulated years per wall-clock day (throughput), and processor layout (total number & root processor in parenthesis) of the different model configurations used in the spinup procedure.

	BG	JG	T
Cost	2800	900	0.3
Throughput	18	75	23,000
Total cores	2160	2772	288
Coupler	1800 (0)	1044 (0)	288 (0)
Atmosphere	1800 (0)	36 (1008)	288 (0)
Land	1476 (0)	756 (0)	288 (0)
River/runoff	1476 (0)	756 (0)	288 (0)
Ice sheet	1800 (0)	2772 (0)	288 (0)
Ocean	360 (1800)	1728 (1044)	288 (0)
Sea ice	288 (1476)	216 (756)	288 (0)
Ocean waves	36 (1764)	36 (972)	288 (0)

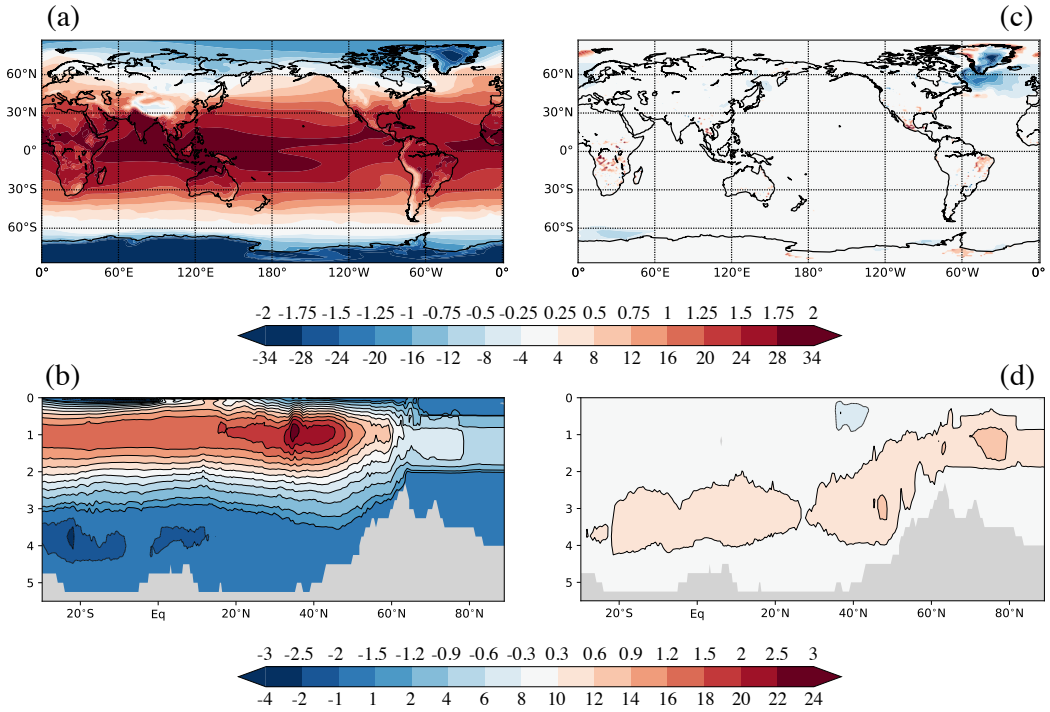

Figure 3. 100-year annual climatologies of: (a) surface temperature [°C]; (b) Atlantic meridional overturning circulation (AMOC) [Sv] from the end of the iterative spinup simulation. Panels c and d show differences with respect to a 100-year climatology from the piControl simulation with a prescribe GrIS geometry. Bottom numbers in colorbar are used by the full fields (panels a and b), and top numbers by the difference plots (panels c and d), respectively. Gray shading in panels b and d indicates the bathymetry. Differences that are not significant at the 99% level are masked out.

Table 2. Comparison of cost and wall-clock time for different ways of running the model. The goal is to run the ice-sheet component 9000 years. BG denotes a fully coupled simulation (BG compset) with a synchronously climate–ice-sheet coupling; BG-10x denotes a BG compset with a 10× ice-sheet model accelerations; JG/BG denotes the iterative spinup procedure. The model cost is given in millions of core hours, and the wall-clock time in days.

	Simulation cost (10^6 core hours)	Wall-clock time (days)
BG	25.2	500
BG-10x	2.52	50
JG/BG	1.68	29

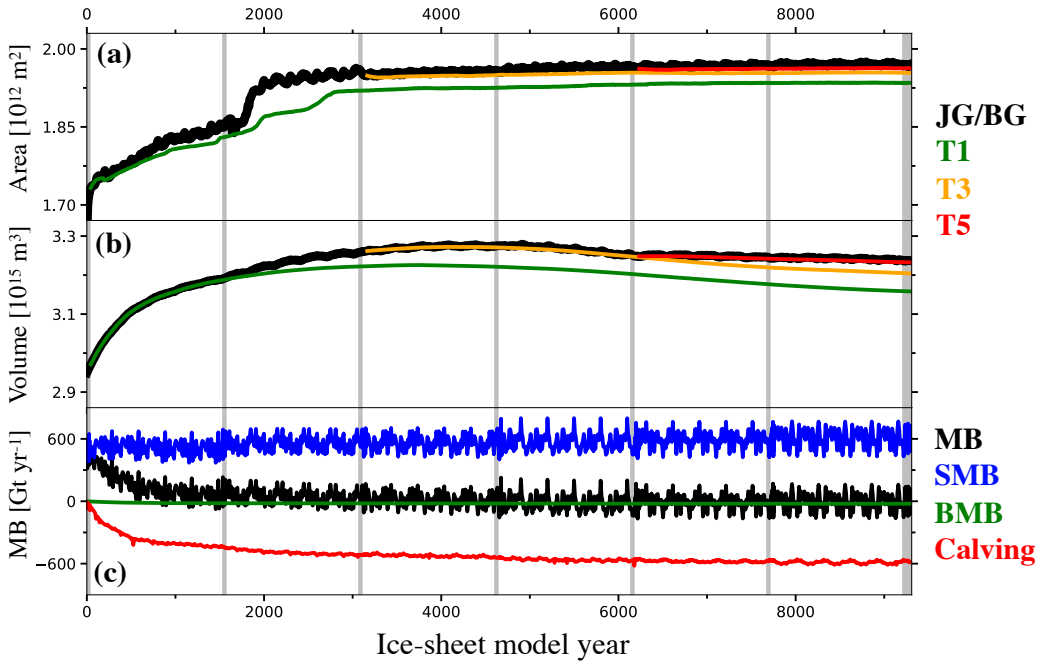

Figure 4. Time evolution of GrIS: (a) area [10^{12} m^2]; (b) volume [10^{15} m^3]; and (c) mass balance (MB; black), surface mass balance (SMB; blue), basal mass balance (BMB; green), and calving (red) [Gt/year]. Black lines in panels (a) and (b) indicate the iterative spinup simulation, and the colored lines are from ice-sheet-only simulations (T compsets). T1 uses forcing data from the first (BG1), T3 from the third (BG3), and T5 from the fifth (BG5) fully coupled segments, respectively. Fully coupled (BG compset) segments are indicated by gray background; JG compset was used elsewhere. Note that the time axis is different from Fig. 2 due to the (10×) ice-sheet acceleration in the JG segments.

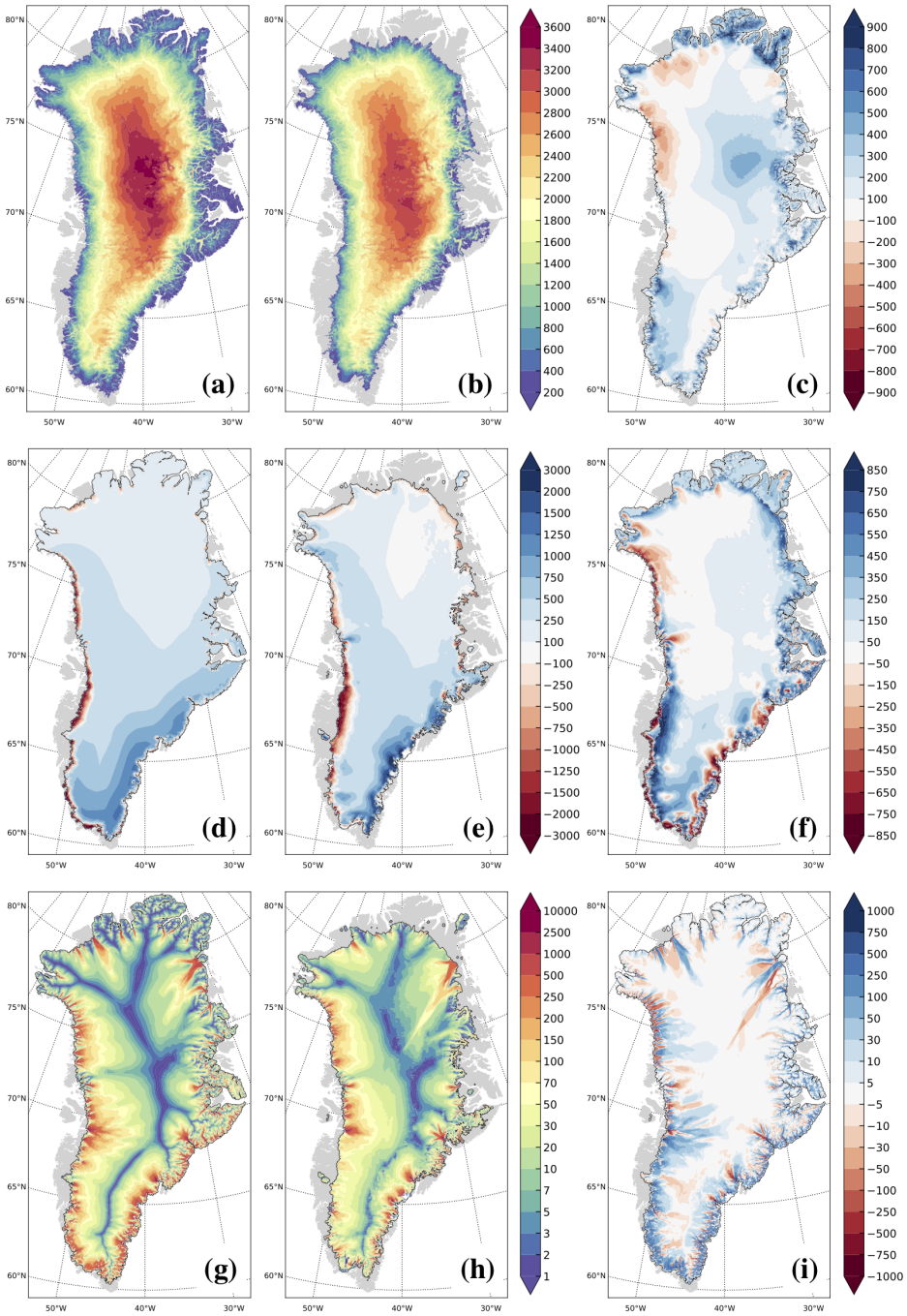

Figure 5. (a) Simulated GrIS thickness [m], (b) observed GrIS thickness (Morlighem et al., 2014), (c) difference between simulated and observed thickness. (d) Simulated surface mass balance [mm w.e. year^{-1}], (e) average surface mass balance between 1960-1989 from RACMO2.3 (Noël et al., 2015), (f) difference between simulation and RACMO2.3. (g) Simulated ice-sheet velocity [m year^{-1}], (g) observed ice-sheet velocity (Joughin et al., 2010), (i) difference between simulated and observed velocities. All fields in the left column are evaluated as 50-year averages from the end of spinup simulation. Gray shading indicates ice-free continent.

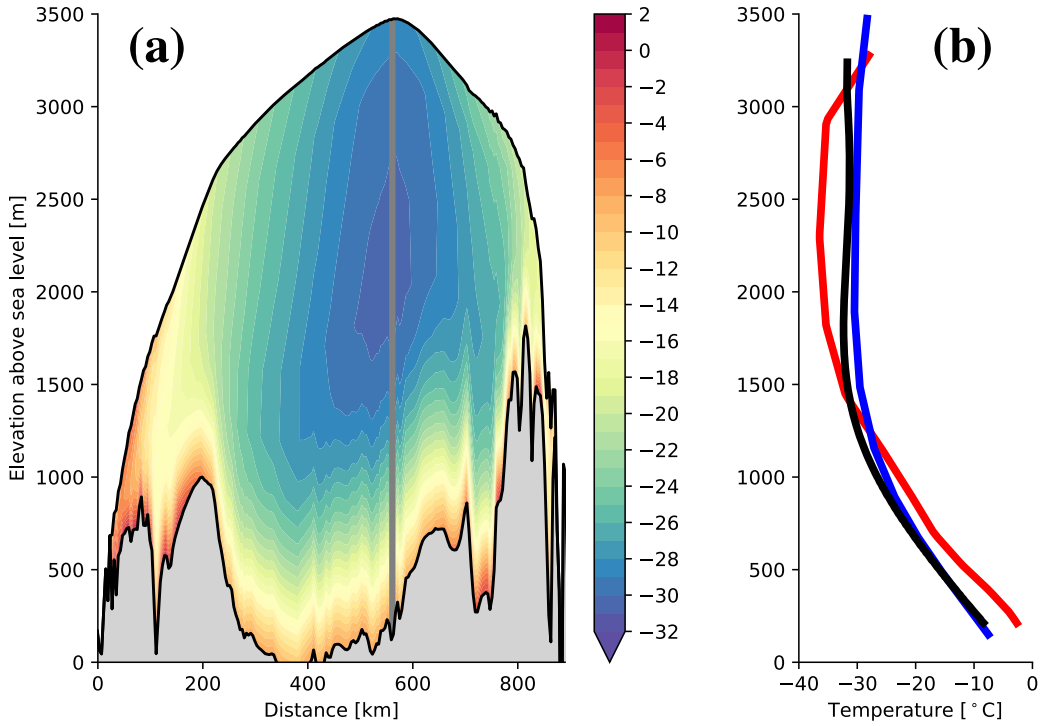

Figure 6. (a) Cross section of temperature [°C] across the central ice sheet at the end of the spinup simulation. (b) Comparison of vertical temperature profiles at summit location (72.6°N, 37.6°W; indicated by gray vertical bar in the left panel) to the GRIP temperature profile; red: temperature from initial conditions (9 ka profile in Fyke et al., 2014); blue: temperature at the end of spinup procedure (the sub-surface cold anomaly is not clearly visible here because of the range on the horizontal axis); black: GRIP temperature profile (Dahl-Jensen et al., 1998).

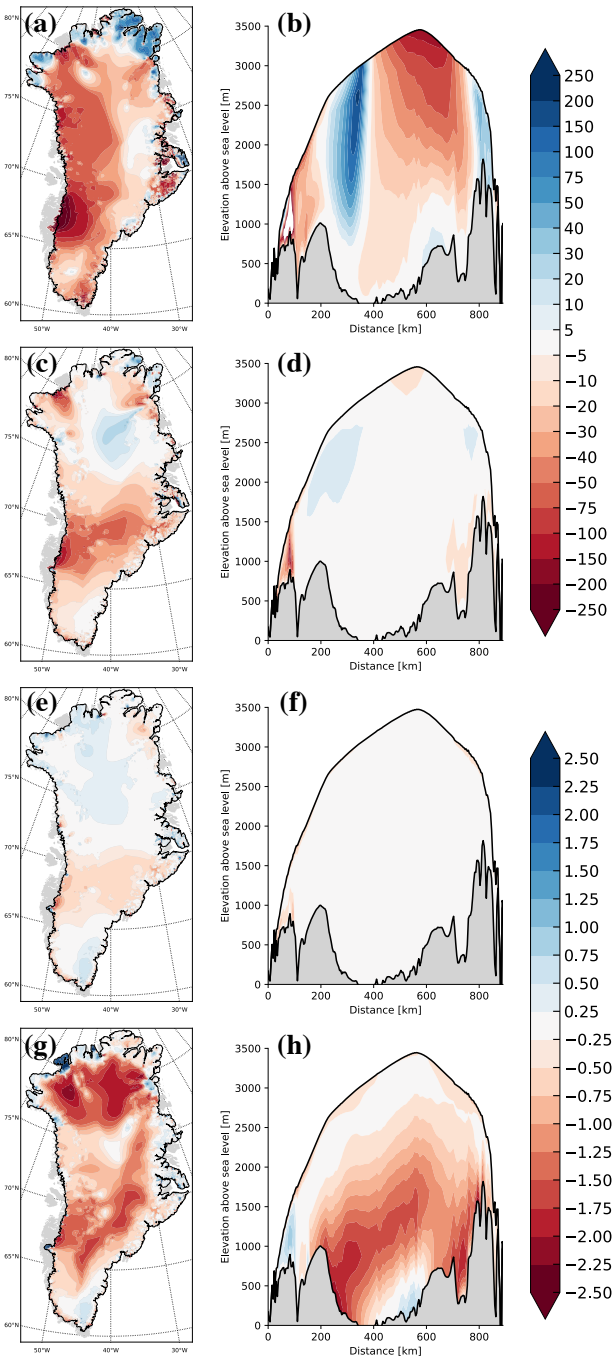

Figure 7. Difference in ice thickness [m] (left) and vertical temperature profile [°C] through the Summit location (right) between the standalone ice sheet model simulations (T compset; see Table 4) and the equilibrated GrIS from the iterative procedure in: (a, b) T1; (c, d) T3; (e, f) T5; and (g, h) T5 extended out 10,000 years beyond the end of the iterative procedure. The top colorbar is used in the left column (panels a,c,e,g), and the lower colorbar is used in the right column (panels b,d,f,h).

Table 3. JG/BG segment average and standard deviation of ice area, ice volume, total mass balance, surface mass balance, calving flux (solid ice discharge), and basal mass balance. The total mass balance is the sum of mass accumulation from surface mass balance, and mass loss from calving fluxes and basal mass balance.

	BG1	JG2	BG2	JG3	BG3	JG4	BG4	JG5	BG5	JG6	BG6	JG7	BG7
Ice-sheet year	35	1535	1570	3070	3105	4605	4640	6140	6175	7675	7710	9210	9310
Ice area $[10^{12}m^2]$	1.705 [0.022]	1.804 [0.034]	1.853 [0.003]	1.929 [0.019]	1.950 [0.001]	1.955 [0.003]	1.956 [0.001]	1.964 [0.003]	1.963 [0.001]	1.968 [0.002]	1.966 [0.001]	1.971 [0.002]	1.968 [0.001]
Ice volume $[10^{15}m^3]$	2.958 [0.005]	3.124 [0.059]	3.192 [0.001]	3.234 [0.019]	3.261 [0.000]	3.272 [0.004]	3.276 [0.000]	3.266 [0.009]	3.248 [0.000]	3.249 [0.002]	3.243 [0.000]	3.242 [0.002]	3.235 [0.001]
Total mass balance [Gt/year]	457 [70]	139 [123]	78 [72]	44 [70]	34 [68]	13 [66]	-4 [81]	-13 [78]	10 [69]	1 [70]	9 [84]	0 [83]	-9 [83]
Surface mass balance [Gt/year]	490 [65]	510 [70]	540 [72]	557 [70]	568 [69]	560 [69]	560 [81]	573 [78]	593 [70]	601 [74]	603 [85]	611 [86]	591 [83]
Calving flux [Gt/year]	-31 [17]	-356 [92]	-443 [5]	-493 [20]	-513 [2]	-526 [11]	-542 [3]	-563 [11]	-560 [2]	-577 [9]	-571 [3]	-587 [13]	-576 [4]
Basal mass balance [Gt/year]	-2 [0.167]	-15 [4.618]	-19 [0.096]	-20 [0.326]	-21 [0.0394]	-21 [0.498]	-22 [0.033]	-23 [0.341]	-23 [0.0282]	-23 [0.151]	-23 [0.056]	-24 [0.299]	-24 [0.076]

Table 4. Volume and area of ice-sheet model simulations (T compset) and the equivalent JG/BG ice sheet year 9410. The standalone ice-sheet model simulations use 30 years of SMB forcing were branched from the each fully coupled segment in the iterative simulation. The T simulations were then run until the nominal ice sheet year matches the end year of the iterative simulation. (T1 was branched from BG1 and was run for 9310 years, T2 branched from BG2 and was run for 7775 years, etc.).

Simulation	Length (Years)	Volume (10^{15} m^3)	Area (10^{12} m^2)
T1	9310	3.16	1.93
T2	7775	3.18	1.96
T3	6240	3.20	1.95
T4	4705	3.20	1.96
T5	3170	3.23	1.96
T6	1635	3.23	1.96
T7	100	3.23	1.96
JG/BG	9310	3.24	1.97